THE JOURNAL OF PHYSICAL CHEMISTRY A

Article

pubs.acs.org/JPCA

Clustering and Photochemistry of Freon CF_2Cl_2 on Argon and Ice Nanoparticles

Viktoriya Poterya,[†] Jaroslav Kočišek,[†] Jozef Lengyel,[†,‡] Pavla Svrčková,[†,‡] Andriy Pysanenko,[†] Daniel Hollas,[‡] Petr Slavíček,[†,‡] and Michal Fárník*[,†]

[†]J. Heyrovský Institute of Physical Chemistry, v.v.i., Academy of Sciences of the Czech Republic, Dolejškova 3, 182 23 Prague 8, Czech Republic

[‡]Department of Physical Chemistry, Institute of Chemical Technology Prague, Technická 5, 166 28 Prague 6, Czech Republic

Supporting Information

ABSTRACT: The photochemistry of CF_2Cl_2 molecules deposited on argon and ice nanoparticles was investigated. The clusters were characterized via electron ionization mass spectrometry, and the photochemistry was revealed by the Cl fragment velocity map imaging after the CF_2Cl_2 photodissociation at 193 nm. The complex molecular beam experiment was complemented by ab initio calculations. The $(CF_2Cl_2)_n$ clusters were generated in a coexpansion with Ar buffer gas. The photodissociation of molecules in the $(CF_2Cl_2)_n$ clusters yields predominantly Cl fragments with zero kinetic energy: caging. The CF_2Cl_2 molecules deposited on large argon clusters in a pickup experiment are highly mobile and coagulate to form the $(CF_2Cl_2)_n$ clusters on Ar_N. The photodissociation of the CF_2Cl_2 molecules and clusters on Ar_N leads to the caging of the Cl fragment. On the other hand, the CF_2Cl_2 molecules adsorbed on the $(H_2O)_N$ ice nanoparticles do not form clusters, and no Cl fragments are observed from their photodissociation. Since the CF_2Cl_2 molecule was clearly adsorbed on $(H_2O)_N$, the missing Cl signal is interpreted in terms of surface orientation, possibly via the so-called halogen bond and/or embedding of the CF_2Cl_2 molecule on the disordered surface of the ice nanoparticles.

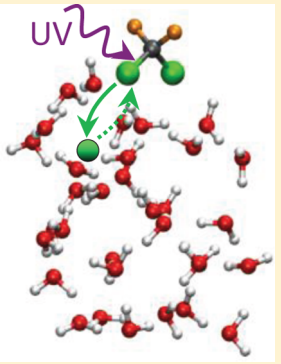

INTRODUCTION

The usage of chlorofluorocarbons (CFC) as refrigerants and foam propellants released a significant load of these molecules into the atmosphere where they affect the atmospheric chemistry.[1−3] In the troposphere, CFCs act as greenhouse gases. They absorb efficiently the radiation in the atmospheric window and have a high global warming potential.[2,4] The CFC molecules are preserved for decades, as relatively inert gases, and they slowly diffuse into the stratosphere, where they can finally be destroyed by solar ultraviolet (UV) radiation. The Cl radical released in the CFC photodissociation initiates the well-known catalytic decomposition of ozone, first proposed by Molina and Rowland.[5] In the present study, we focus on the interaction and photodynamics of dichlorodifluoromethane CF_2Cl_2 (CFC-12) with nanoparticles.

Many of the important stratospheric processes take place on the surface of ice particles in the polar stratospheric clouds (PSC).[1,6] It is therefore relevant to ask whether the photochemistry of CFCs can be controlled by their adsorption on ice surfaces. The CFC molecules adsorbed on ice have also received a significant attention in connection with reactions of presolvated electron. The dissociative electron attachment to CFC-12 in the gas phase[7] increases by several orders of magnitude upon the adsorption on ice for electrons with near-zero kinetic energy, as reported by Lu et al.[8,9] This mechanism has been proposed as an additional potential source of Cl radicals in the stratosphere.[10,11] Interestingly in the context of the present work, the high-energy resonances associated with the excited states of CFCs disappear upon the transition from the gas phase to a polar solvent.[12,13]

To the best of our knowledge, no experiment on the UV-photodissociation of CF_2Cl_2 on ice has been reported so far. Similar chlorine containing molecules, such as $CFCl_3$, have been studied, and their photodissociation dynamics revealed by the time-of-flight (TOF) spectroscopy of Cl fragments released from the ice surface.[14,15] Chemical reactions of CFC-12 in water ice films have been investigated upon X-ray or electron irradiation of the ice.[16,17]

A CF_2Cl_2 molecule absorbs UV-photons with wavelengths below $\lambda \approx 225$ nm and undergoes a direct photodissociation of a single C−Cl bond:

$$CF_2Cl_2 \rightarrow CF_2Cl\cdot + Cl\cdot \quad (1)$$

Photodissociation dynamics of CFC-12 in the gas phase at 193 nm was investigated previously,[18−20] and the quantum yield measurements were reported by Taketani et al.[21] Recently, we have implemented the up-to-date velocity map imaging (VMI) technique to study the detailed photodissociation dynamics of CF_2Cl_2[22] and compared our results with the previous TOF measurements of Baum and Huber[19] and Yen et al.[20] Within the same work, we have investigated the CFC-12 photo-dissociation embedded in rare gas clusters.[22] Here we extend

Received: April 23, 2014
Revised: June 3, 2014
Published: June 9, 2014

   dx.doi.org/10.1021/jp503983x | J. Phys. Chem. A 2014, 118, 4740−4749

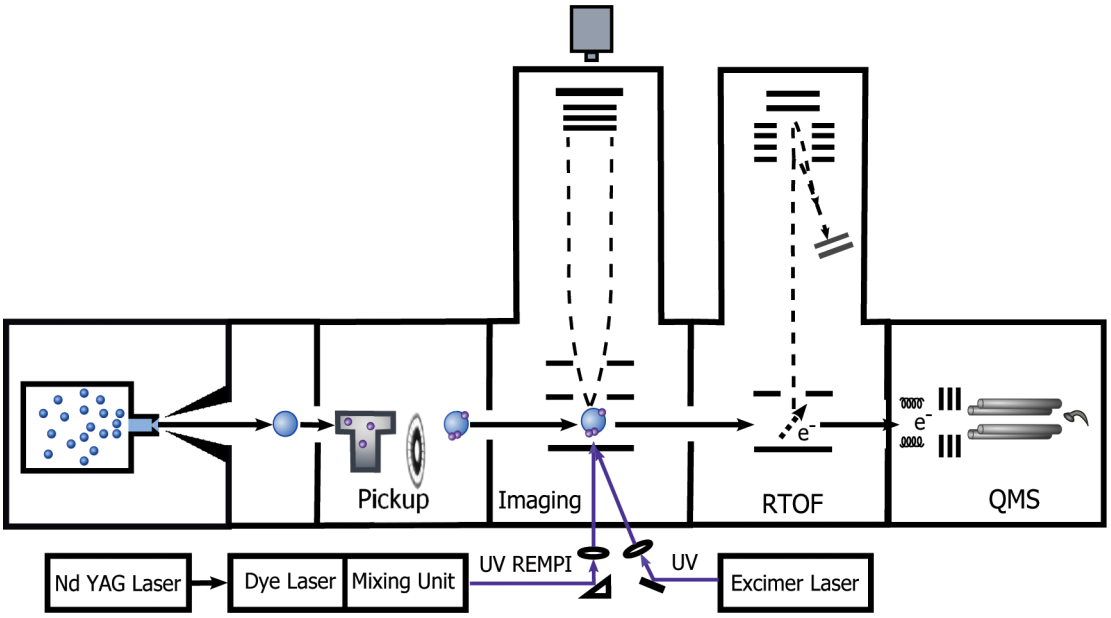

Figure 1. Schematic drawing of the CLUster Beam (CLUB) apparatus outlining the experiments exploited in this paper.

Table 1. Expansion Conditions: Nozzle Diameter was 55 μm for CFC-12 and Ar Expansions, and 100 μm for Water; Divergence Angle was 30° and Thickness 2 mm for all Expansions; Nozzle Temperature, and Stagnation Pressure P_0 [for Water P_0 was Determined by the Water Reservoir Temperature (T_R)][a]

expansion gas	source temperature T_0/T_R (°C)	pressure P_0 (bar)	generated species	mean size $\bar{N}$	pickup P_{CFC} (10^{-4}mbar)
CFC-12	+40	0.5−1.7	CF_2Cl_2	1	−
CFC-12/Ar	+40	0.5−1.7	$(CF_2Cl_2)_n$	1−16	−
Ar	−60 − −40	5.0−8.0	Ar_N	200−450	0.1−5.5
H_2O	+155−170/130−160	3.5−7.7	$(H_2O)_N$	200−750	0.1−5.5

[a]Mean cluster sizes $\bar{N}$ for Ar_N and $(H_2O)_N$ clusters were calculated using Hagena's and Buck's formulas.[41−45] For $(CF_2Cl_2)_n$ clusters, the range of the observed fragments in the mass spectra is given.

our previous studies to the systems where the CFC-12 molecules were deposited on surfaces of large Ar_N clusters, and on atmospherically relevant ice nanoparticles.

In the present study, we continue in our long-term effort to understand how the environment affects the photoinduced processes. They can range from purely mechanical trapping of the molecular fragments formed within the photodissociation, cage effect,[22−24] to complex processes involving reactions of the dopant with the surface.[25−28] The CFC-12 molecule represents an interesting example in this context. The photodissociated Cl fragment can dissipate its kinetic energy efficiently because of its higher mass comparable to the cluster constituents. Thus, it is a more sensitive probe of the interactions in the excited state than the hydrogen fragment investigated in our previous studies. The CFC-12 molecule is also anisotropic. We might ask whether and how the molecule is oriented on the ice surface. The preferential orientation could be mediated by the so-called halogen bond[29] between the CF_2Cl_2 and water, C−X···OH_2 (X = Cl and F).

The experimental arrangement used for the study is unique since it combines several experimental tools in one apparatus: (1) well-defined production of relatively large clusters (nanoparticles);[30] (2) investigation of the photodissociation dynamics with the velocity map imaging (VMI) method;[22,24] (3) high-resolution mass spectrometry after electron ionization for the cluster composition determination;[31,32] and (4) pickup experiment for cluster size determination.[33−35] In the present work, we have combined all these methods for the first time to deliver a complex picture of the investigated cluster species and processes in their environment.

EXPERIMENTAL AND THEORETICAL METHODS

Experiment. Figure 1 shows the schematic overview of the present experiments. The general description of our CLUster Beam apparatus (CLUB) can be found elsewhere.[30,36] Recently, the experiment has been extended with the velocity map imaging (VMI) technique and a reflectron time-of-flight mass spectrometer (RTOF). The combination of these techniques within one apparatus can provide a detailed insight into the studied cluster species and processes.

Various clusters were produced under different expansion conditions, which are summarized in Table 1. The expansion was skimmed ∼25 mm downstream from the nozzle, and the beam passed about 1 m through two differentially pumped chambers into the detection VMI chamber where the photodissociation of molecules in clusters was investigated. The VMI system is perpendicular to the beam axis, and the design is identical to our other apparatus for imaging (AIM) described in more detail elsewhere.[22,24,37] For the position sensitive detection, we used chevron multichannel plate (TOPAG) with an active diameter of 41 mm in combination with P43 phosphor screen and CCD camera (Unibrain Fire-i 702b) with imaging lens (25 mm, f/1.6). To process the images the inverse Abel transform was performed. We used the Hankel

dx.doi.org/10.1021/jp503983x | J. Phys. Chem. A 2014, 118, 4740−4749

method for reconstructing the images,[38] and also the Iterative Inversion method[38] was implemented to check the consistency of our results.

In the interaction point, the molecular beam was crossed with two laser beams: the photodissociation 193.3 nm ArF-Excimer laser and 235.336 nm laser to REMPI ionize the $Cl(^2P_{3/2})$ photofragments. The tunable UV radiation around 235 nm is generated by sum frequency mixing of the fundamental 1064 nm from the Nd:YAG laser (Spitlight 1500, Innolas) with the doubled output of the tunable dye laser (Pulsare-S, Lioptec) pumped by the Nd:YAG second harmonics (532 nm). The pulsed lasers were crossed under the mutual angle of 17.5° and operated at a 10 Hz frequency in the nanosecond regime.

The next vacuum chamber was hosting the RTOF mounted orthogonally to the molecular beam. It was custom-built on the basis of our specifications[39] and described in detail in our recent studies.[32,40] The clusters were ionized by electrons at 10 kHz repetition frequency, and the mass spectra of the ionized product were recorded with the resolution of $(M/\Delta M) \approx 10^4$. The present spectra were recorded at the electron energy of 70 eV.

Finally, the quadrupole mass spectrometer at the end of the machine was used for the velocity measurements. The cluster beam was interrupted with a pseudorandom chopper after the pickup process, and the time-of-flight was recorded after the clusters were ionized by electrons in the quadropole ion source and a particular ion fragment detected. The cluster velocity was evaluated from the flight time. Measuring the cluster velocity as a function of the gas pressure in the pickup chamber allowed for the evaluation of the cluster cross section for the pickup of molecules. The velocity measurements and cluster cross section determination methods have been outlined in detail in our recent publications.[33−35]

This has been the very first study performed on our CLUster Beam (CLUB) apparatus in which we combined the different experiments: (i) the high resolution time-of-flight mass spectrometry, (ii) the photofragment velocity imaging, and (iii) the pickup cross-section measurements.

Theory. The interpretation of our measurements has been assisted by ab initio calculations. We have calculated the geometries of the participating molecules and structures of the respective binary complexes between CFC-12, water, and argon. The structures of the complexes were optimized at the MP2 level with cc-PVTZ basis. The counterpoise correction of Boys and Bernardi was employed during the optimization.[46] Such a combination has been shown to provide highly accurate geometries for van der Waals complexes.[47] The binding energies were then calculated within a supramolecular approach at the CCSD(T)/CBS level. The procedure was as follows. First, the MP2/CBS energy was obtained by extrapolating the aug-cc-pVTZ- and aug-cc-PVQZ-based calculations to the complete basis set limit using the n^{-3} formula. The HF energy was not extrapolated but taken from the calculation with the aug-cc-pVQZ basis set. The CCSD(T) correction to the MP2 result was computed with the aug-cc-pVDZ basis and added to the MP2/CBS energy. The final energy expression thus reads:

$$E_{\mathrm{CBS}}^{\mathrm{CCSD}(T)} = E_{\mathrm{aug-pVQZ}}^{\mathrm{HF}} + E_{\mathrm{CBS}}^{\mathrm{RI-MP2}} + E_{\mathrm{aug-pVDZ}}^{\mathrm{CCSD}(T)} - E_{\mathrm{aug-pVDZ}}^{\mathrm{MP2}} \quad (2)$$

This scheme has been shown to be of a comparable accuracy to more costly direct extrapolation of CCSD(T) energies.[48] The counterpoise correction was also used for the binding energy calculations.

We have also investigated the excited states of the CFC molecule in the gas phase and in the binary complexes. The high-level estimates of the excitation energies and corresponding oscillatory strengths were performed with the EOM-CCSD method, using aug-cc-pVTZ basis set. The mapping of the excited state potential energy surface along the C−Cl dissociation coordinate was performed with multi reference configuration interaction (MRCI) method with single and double excitations. The CI treatment was performed on the complete active space self consistent fields (CASSCF) wave function defined by 8 electrons distributed in 5 active orbitals. This choice has provided a consistent description of the potential energy surface (PES) of both isolated CFC and CFC complexed with water and argon.

Most of the calculations were performed in Molpro, version 2010.[49,50] The optimization of the binary complexes with the counterpoise correction was done in Gaussian09.[51]

RESULTS AND DISCUSSION

Our major target was the atmospherically relevant photochemistry of CF_2Cl_2 on ice nanoparticles. To meet this aim, we have investigated the photodissociation gradually proceeding from the isolated molecule to the photodissociation in the environment of $(CF_2Cl_2)_n$ and rare gas clusters and finally in $(H_2O)_N$. This section is structured as follows: first, we demonstrate (namely by mass spectrometry) and discuss the generation of the different clusters in our experiment; second, the VMI results of photodissociation experiment are presented and discussed; and third, the surprising disappearance of Cl fragment from photodissociation on ice nanoparticles is discussed and justified in more detail.

Nature of Generated Clusters Species. *Coexpansion with Ar.* The CF_2Cl_2 molecules do not generate clusters in pure expansions: figure 2a shows an example of the mass spectrum measured at P_0 = 1.7 bar CF_2Cl_2 expansion pressure and T_0 = 50 °C nozzle temperature exhibiting only fragments of isolated CF_2Cl_2 molecule. Figure 2b corresponds to the expansion of 10% CFC in Ar under the same stagnation conditions. The inset shows that ionized fragments of $(CF_2Cl_2)_n$ clusters even for $n \geq 16$ have been observed. There are three groups of cluster fragment ions corresponding to each size n: $(CF_2Cl_2)_n^+$ cluster ions composed of nonfragmented molecules, and $CFCl_2(CF_2Cl_2)_{n-1}^+$ and $CF_2Cl(CF_2Cl_2)_{n-1}^+$ cluster ions where F or Cl atom, respectively, was missing. The individual mass peaks in each group correspond to various combinations of ^{35}Cl and ^{37}Cl isotopes as confirmed by their intensity ratios. Indeed, these fragment ions can originate from any neutral cluster size $\geq n$. Since no mixed CF_2Cl_2/Ar fragments were observed in the coexpansion mass spectra, we propose that pure $(CF_2Cl_2)_n$ clusters were generated. This will be contrasted to CF_2Cl_2 deposited on the Ar_N surface discussed below. Additional spectra showing the expansion pressure dependence are shown in the Supporting Information.

The fact that no clusters were generated in the pure CF_2Cl_2 expansions demonstrates that the molecule itself is very inefficient for cooling the expansion. On the other hand, the $(CF_2Cl_2)_n$ clusters were readily generated in the coexpansion with Ar. We can briefly discuss the cluster formation in terms of the calculated binding energies of binary complexes summarized in Table 2. The $CF_2Cl_2\cdots CF_2Cl_2$ binding energy is higher than for the $CF_2Cl_2\cdots$Ar and Ar···Ar complexes. Thus, argon

dx.doi.org/10.1021/jp503983x | J. Phys. Chem. A 2014, 118, 4740−4749

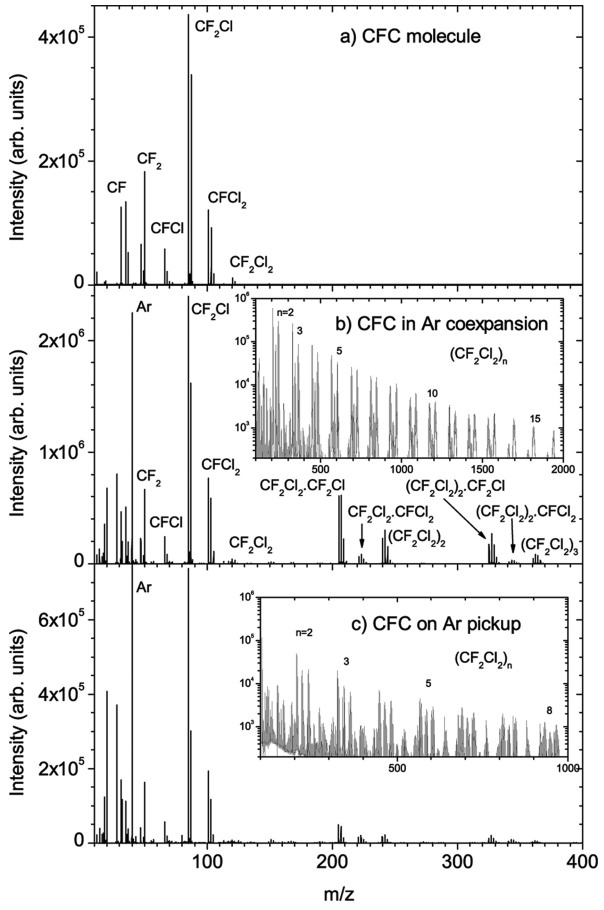

Figure 2. Electron ionization (70 eV) mass spectra (TOFMS): (a) pure CF_2Cl_2 molecule expansion P_0 = 1.7 bar, T_0 = 50 °C, and molecular fragments indicated. (b) Expansion of 10% CFC in Ar, P_0 = 1.7 bar, T_0 = 50 °C, and fragments of $(CF_2Cl_2)_n$ clusters indicated; the inset shows clusters from n = 2 up to 17 (note the logarithmic scale). (c) Pickup of CF_2Cl_2 molecules on Ar_N, $\bar{N}$ = 330, expansion conditions: P_0 = 7.5 bar, T_0 = −50 °C, and CF_2Cl_2 pressure in the pickup chamber $P_{CFC} = 5.2 \times 10^{-4}$ mbar; the inset shows clusters from n = 2 up to 8.

atoms serve as an efficient cooling medium in the expansion; they take away the excess energy released upon the CF_2Cl_2 aggregation and do not bind to the clusters.

Pickup on Large Ar Clusters. In the second series of experiments, pure Ar_N clusters were generated and the CF_2Cl_2 molecules were deposited on them in the pickup chamber. It ought to be mentioned that pure rare gas expansions were investigated in great detail previously,[41−44] and the cluster size distributions are well-known. In our experiments, the species were probed more than a meter downstream from the source, where the molecular beam was well-defined, and the clusters were stabilized after almost 1 ms flight-time in vacuum. Different expansion conditions were exploited corresponding to different cluster sizes and also different CF_2Cl_2 pressures in the pickup cell. The conditions and corresponding cluster sizes are summarized in Table 1. At lower pickup pressures, the spectra were dominated by the Ar_N^+ series. Increasing the CF_2Cl_2 pressure yielded $(CF_2Cl_2)_n$ clusters built after multiple CF_2Cl_2 pickup on Ar_N clusters. Figure 2c shows the mass spectrum at a high pickup pressure $P_{CFC} = 5.2 \times 10^{-4}$ mbar, where the mass peaks corresponding to $(CF_2Cl_2)_n$ clusters dominate over Ar_N^+. Further spectra illustrating the pressure dependence can be found in the Supporting Information.

The spectrum in Figure 2c is similar to the spectrum obtained in the coexpansion (b). Yet, closer inspection reveals some differences, namely the presence of the mixed CF_2Cl_2/Ar ions in (c). This is demonstrated in Figure 3, where a detailed

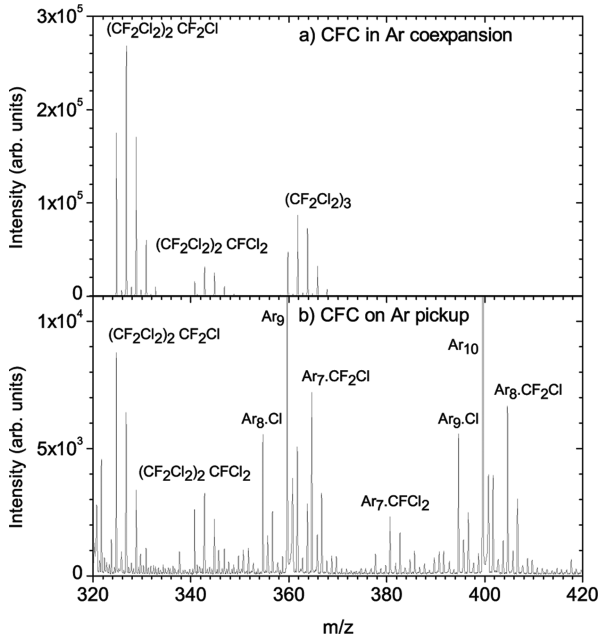

Figure 3. Detailed section of the mass spectrum from (a) expansion of CFC mixture in Ar (P_0 = 1.7 bar, T_0 = 57 °C), in comparison with (b) pickup of CF_2Cl_2 molecules on Ar_N clusters (P_0 = 8 bar, T_0 = −59 °C, $P_{CFC} = 7.4 \times 10^{-5}$ mbar).

part of the (a) coexpansion spectrum is compared to the (b) pickup spectrum at somewhat lower pickup pressure of P_{CFC} = 7.4×10^{-5} mbar to show clearly the Ar-series mass peaks. The spectrum is dominated by Ar_N^+ and exhibits the mixed mass peaks Ar_NCl^+, $Ar_NCF_2Cl^+$, and $Ar_NCFCl_2^+$, in addition to the CF_2Cl_2 cluster series: $(CF_2Cl_2)_n^+$, $CFCl_2(CF_2Cl_2)_{n-1}^+$, and $CF_2Cl(CF_2Cl_2)_{n-1}^+$.

These spectra recorded in the pickup experiment under various conditions have provided the experimental evidence that CF_2Cl_2 molecules are adsorbed and coagulate to the $(CF_2Cl_2)_n$ clusters on the Ar_N clusters. The Ar_N cluster absorbs the CF_2Cl_2 binding energy, subsequently disposing it by the Ar evaporation. The binding energy of $(CF_2Cl_2)_2$ dimer is approximately 90 meV, according to our calculations. Presumably, CF_2Cl_2 will be bound by somewhat higher energy in larger clusters: four-times the dimer energy can be assumed as the upper boundary (i.e., ∼360 meV). From the mass spectra, $n \leq 10$ corresponds to the largest size of the $(CF_2Cl_2)_n$ cluster generated on the Ar_N at the highest pickup pressure.

Table 2. Calculated Binding Energies of Various Binary Complexes at the Estimated CCSD(T)/CBS Level

complex	$CF_2Cl_2\cdots CF_2Cl_2$	$CF_2Cl_2\cdots H_2O$	$CF_2Cl_2\cdots Ar$	$H_2O\cdots H_2O$	$Ar\cdots Ar$
ΔE_{int} (meV)	87	88	35	218[53]	12[54]

dx.doi.org/10.1021/jp503983x | J. Phys. Chem. A 2014, 118, 4740−4749

Therefore, the total energy of ~3600 meV can be released by the CFC-12 coagulation at most. The binding energy of Ar to Ar_N is approximately 60 meV for $N = 200$.[52] Thus, the CFC-12 coagulation evaporates less than 60 Ar atoms. This number is smaller than the smallest investigated mean Ar_N cluster size $\bar{N} \approx 200$. Therefore, in the pickup experiments, small $(CF_2Cl_2)_n$ clusters were generated on the surface of large Ar_N clusters, where n ranges from 1 (single molecule pickup) to ~10 and $N > 10 \times n$.

In this case, argon again represented an efficient heat bath promoting the CF_2Cl_2 aggregation. In the pickup process, the energy released by the CF_2Cl_2 clustering was not sufficient to evaporate the large argon cluster and mixed $(CF_2Cl_2)_n{\cdot}Ar_N$ species were generated. It is interesting to note that the CF_2Cl_2 molecules must be highly mobile on the argon surface to coagulate after the uptake.

Pickup on Ice Nanoparticles. In the last series of experiments, we deposit the CF_2Cl_2 molecules on large water clusters $(H_2O)_N$ generated in water vapor expansion. As for argon clusters, the water cluster size distributions were investigated and characterized in great detail, in this case even with our present cluster source.[45] The present experiments were done with different mean water cluster sizes between $\bar{N} \approx 200$ and 750 and various CF_2Cl_2 pickup pressures, as in the case of Ar_N clusters (Table 1). Figure 4

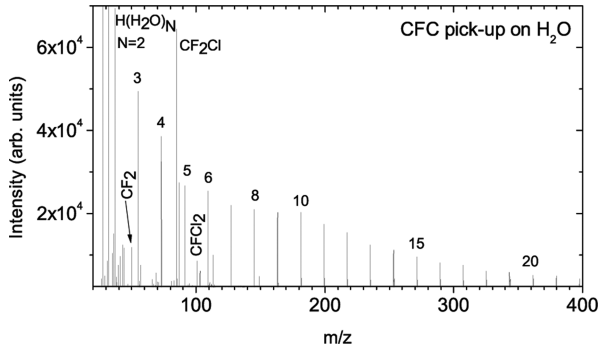

Figure 4. Mass spectrum from pickup of CF_2Cl_2 molecules on $(H_2O)_N$, $\bar{N} \approx 750$ clusters, $P_{CFC} = 2.5 \times 10^{-4}$ mbar.

shows an example mass spectrum for $\bar{N} \approx 750$ with the series of protonated clusters $(H_2O)_NH^+$ typical for the water cluster ionization. The only ions corresponding to CF_2Cl_2 molecules identified in the spectra were the strong CF_2Cl^+ peak and substantially weaker, yet discernible, CF_2Cl^+ and CF_2^+. There was no evidence for CF_2Cl_2 clusters nor for mixed CF_2Cl_2/H_2O fragments under any exploited conditions.

It ought to be stressed that the background spectrum of any diffused CF_2Cl_2 molecules was carefully subtracted, and the relatively strong CF_2Cl^+ peak appeared only due to the ionization of the CF_2Cl_2 molecules arriving to the mass spectrometer with the $(H_2O)_N$ clusters. Since there is no evidence for $(CF_2Cl_2)_n$ clusters on $(H_2O)_N$, the CF_2Cl_2 molecules were either less mobile on the ice than on argon or did not bind even if they met on the $(H_2O)_N$ surface, or there were fewer molecules adsorbed on ice than on argon. The two former options are supported by our calculations. The $CF_2Cl_2{\cdots}H_2O$ interaction is much stronger than the corresponding $CF_2Cl_2{\cdots}Ar$ interaction. The mobility of the molecule is thus limited. At the same time, the $CF_2Cl_2{\cdots}CF_2Cl_2$ interaction is weaker than for $CF_2Cl_2{\cdots}H_2O$. Thus, there is no reason for a preferential coagulation of the CF_2Cl_2 molecules on the ice surface.

To answer the question if there are less CF_2Cl_2 molecules deposited on the ice nanoparticles than on Ar_N, we have performed an additional experiment: the pickup cross-section measurements. The geometrical size of the investigated water and argon clusters was comparable. The radius of the clusters can be estimated as $R = R_0{\cdot}N^{1/3}$, where the parameter R_0 can be evaluated from the density ρ as $R_0 = [(3/4\pi)(m/\rho N_A)]^{1/3}$, m is the molar mass, and N_A is Avogadro's constant. Solid argon and water ice densities yield $R_0 = 2.09$ and 1.93 Å, respectively. This implies that $M/N \approx 1.3$ for $(H_2O)_M$ and Ar_N clusters of the same radius. We investigated clusters from the corresponding size range, however, the sticking of the CF_2Cl_2 molecules to $(H_2O)_M$ and Ar_N clusters can be different. In the present experiments, we determine the pickup cross section $\sigma \approx 1000$ Å^2 for CF_2Cl_2 molecules on Ar_N, $\bar{N} = 330$, using our recently developed method based on cluster velocity measurements.[33−35] The measured cross section corresponds to approximately 20 CF_2Cl_2 molecules deposited on Ar_N at the highest exploited pressure $P_{CFC} = 5.2 \times 10^{-4}$ mbar (the mass spectra exhibited ionized fragments up to about $n \approx 10$). The measured pickup cross section for the CF_2Cl_2 molecules on $(H_2O)_M$, $\bar{M} = 430$, was about 4 times smaller. Nevertheless, multiple pickup of about 5 CF_2Cl_2 molecules is still expected on $(H_2O)_M$ under the same conditions as for Ar. Even more adsorbed molecules is expected on the larger clusters (up to $\bar{M} \approx 750$), which we investigated. Yet, a possible evaporation of CF_2Cl_2 molecules should be considered as discussed below.

In all cases, the presence of the CF_2Cl_2 peak in the mass spectra proved that the ice nanoparticles arrive into the photodissociation region with one or more nonclustered CF_2Cl_2 molecules.

Photodissociation in Clusters. Here we present the VMI results for the different cluster species, which were produced as

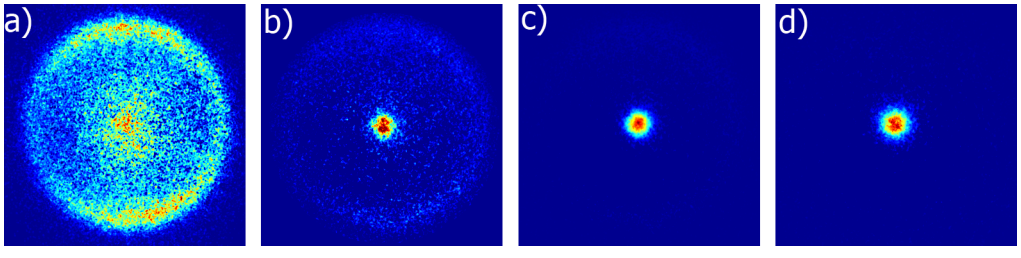

Figure 5. Cl-fragment images from 193 nm photodissociation of CF_2Cl_2 in various environments (laser polarization vertical): (a) isolated CF_2Cl_2 molecules; (b) $(CF_2Cl_2)_n$ clusters generated in CFC/Ar expansion at $P_0 = 1.4$ bar, and (c) 1.7 bar; (d) CF_2Cl_2 molecules deposited on large Ar_N clusters.

dx.doi.org/10.1021/jp503983x | J. Phys. Chem. A 2014, 118, 4740−4749

outlined in the previous section. Figure 5 shows the Cl fragment images for the various cases.

CF_2Cl_2 Molecule. The image in Figure 5a corresponds to the photodissociation of the isolated CF_2Cl_2 molecule. Similar images have been recorded in expansions of pure CFC-12 and also in expansions of CFC/Ar mixtures below 1 bar stagnation pressure. These images agree with our recent study[22] performed on AIM and were analyzed in detail there. Here we repeat only the major conclusions for the sake of completeness. The underlying reason for the lower signal-to-noise ratio in the present image is a very long (>1 m) flight path from the source to the laser interaction region in CLUB compared to AIM (~10 cm). The long flight path reduces the monomer intensity, yet it brings advantages for large cluster studies. The kinetic energy distribution (KED) shown in Figure 6 is dominated by the fast fragments at $E_{kin}(Cl)$ = 0.97 eV

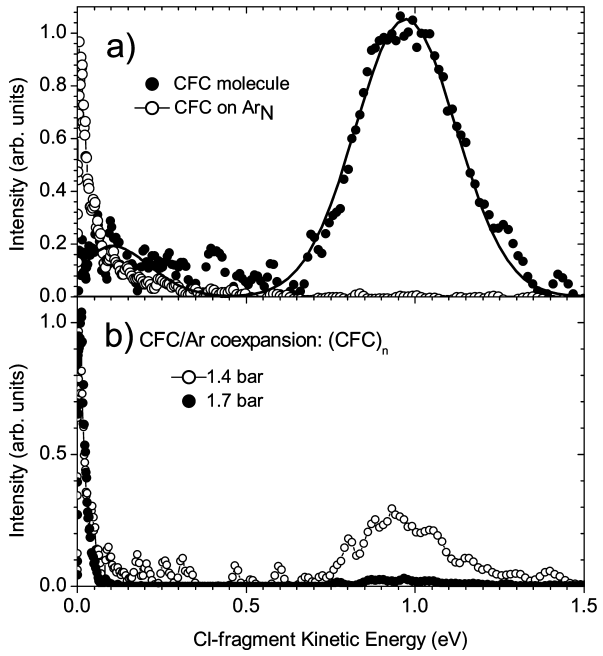

Figure 6. Cl-fragment KEDs: (a) isolated CF_2Cl_2 molecules (●) and CF_2Cl_2 molecules deposited on large Ar_N clusters (○); (b) $(CF_2Cl_2)_n$ clusters generated in CFC/Ar expansion at 1.4 bar (○) and 1.7 bar (●).

originating from the direct Cl−CF_2Cl bond fission at 193 nm. Additionally, there are some slower fragments below ~0.5 eV, which were also identified in the earlier work of Yen et al.[20] These slow fragments can be formed in the concerted dissociation of the two Cl atoms from CF_2Cl_2; in the secondary CF_2Cl dissociation; or due to multiphoton processes. For the discussion see our previous study;[22] here, we concentrate on how the dynamics of the process changes in the clusters.

$(CF_2Cl_2)_n$. First, we probed pure $(CF_2Cl_2)_n$ clusters generated in mixed expansions. The images in Figure 5, (panels b and c) show an increasing contribution of the caged Cl fragments (in the middle) compared to the fast Cl-fragments, corresponding to the direct exit from clusters. The fast fragments disappeared almost entirely at the higher expansion pressure of P_0 = 1.7 bar; see also the corresponding KEDs in Figure 6b. Even for the larger $(CF_2Cl_2)_n$ clusters where the caging strongly dominates, some direct exit fragments are still discernible in the KED (Figure 6b). The rapid disappearance of the fast velocity component with increasing cluster size reflects the efficient dissipation of energy of the dissociated chlorine fragment. Several collisions suffice to essentially stop the chlorine atom. The caging is thus rather efficient even in medium-sized $(CF_2Cl_2)_n$ clusters. In contrast, caging of the hydrogen atom in hydrogen halide clusters of similar sizes[55−57] was less pronounced.

The pattern corresponding to the fast fragments in the images from clusters exhibited slightly lower anisotropy than the fast fragments from isolated molecules. The more isotropic distribution could be caused by the elastic scattering of the Cl fragments in the cluster. Yet, the differences in the anisotropy parameter β were within the error bars of the limited signal intensities. Thus, we cannot determine unambiguously whether the fast fragments in the cluster images originated from the clusters or unclustered molecular fraction in the beam.

$(CF_2Cl_2)_n \cdot Ar_N$. Figure 5d shows an example of the image from Ar_N clusters with the CF_2Cl_2 molecules deposited on their surface. The corresponding KED is compared to the molecular spectrum in Figure 6a. At lower pickup pressures (where the mass spectra indicated that only a single CF_2Cl_2 molecule was deposited on the Ar_N cluster), a weaker Cl signal corresponding to Cl caging is still clearly observed. However, its low intensity prevents to unambiguously distinguish any faster fragments at the position of the direct exit peak from the background. Thus, essentially only the caged Cl fragments were observed from the CF_2Cl_2 photodissociation on Ar_N. On the other hand, for the H-fragment from hydrogen halides deposited on rare gas clusters, some cage exit has been observed previously.[23,58−61] The mass of the argon atom is close to the mass of the chlorine fragment, and thus it very efficiently slows the chlorine upon collisions.

$CF_2Cl_2 \cdot (H_2O)_N$. Finally, we performed the photodissociation experiment on the large water clusters with the CF_2Cl_2 molecules deposited on them by the pickup. Despite the fact that we observed the CF_2Cl_2 molecules deposited on the $(H_2O)_N$ clusters in the mass spectrometry experiment (as outlined in the previous section), we did not obtain any Cl signal from its photodissociation under any exploited experimental conditions (Table 1). It is a negative yet important result, and we discuss it in more detail in the next section.

Rationalization of the Chlorine Fragment Disappearance. In this section, we discuss the possible explanations for the lack of the chlorine signal upon the photodissociation of the CF_2Cl_2 molecule on the surface of ice nanoparticles. Several options can be outlined: (1) the CF_2Cl_2 molecule is not present in the photodissociation region in sufficient quantity, (2) the molecule is not photoexcited at 193 nm, or (3) the excitation does not yield the free chlorine radical.

(1). Small Amount of CF_2Cl_2. The trivial reason for the lack of the signal could be the small amount of CF_2Cl_2 molecules adsorbed on the $(H_2O)_N$ clusters. It has been reported previously[62] that CFC-12 begin to desorb from the ice surface at temperatures above approximately 100 K, but they can be trapped inside the ice film up to the temperature of about 150 K. The temperature of the water clusters is typically estimated to be around 100 K; however, the exact value is not known and a range of temperatures between 80 and 150 K can be found in the literature.[63−65] The desorption from finite size clusters should be considered in the context of time available between the pickup and photodissociation. The desorption rate constant can be estimated as

dx.doi.org/10.1021/jp503983x | J. Phys. Chem. A 2014, 118, 4740−4749

$$k = \nu \exp(-E_a/k_B T) \quad (3)$$

where E_a is the activation barrier which can be in first approximation identified with the binding energy. The attempt frequency ν is typically considered 10^{12} s^{-1}.[66] If a binding energy of the CFC-12 on ice[67] is around 0.3 eV, the desorption lifetime is in the order of minutes for 100 K. This is well above the ≈0.6 ms time interval between the pickup and the photodissociation events. The CFC-12 molecule should stay on the ice particle for the time required even at 150 K. This conclusion is consistent with the relatively strong CF_2Cl^+ peak in the mass spectra, which can be only due to the molecules arriving with the clusters to the detector, as argued above. The pickup cross section measurements above suggest that there are less CF_2Cl_2 molecules adsorbed on $(H_2O)_N$ than on Ar_N. Yet, the signal from the pickup on Ar_N was relatively strong, and the signals more than an order of magnitude lower would still be distinguished from the background.

(2). Shift in the Absorption Spectra. The water solvent molecules could influence the CF_2Cl_2 photoabsorption cross section on the ice nanoparticle. Blue shift of the spectrum could lead to a lower probability of the absorption at 193 nm (6.41 eV). Our calculations showed, however, little influence of the water solvent on the CF_2Cl_2 absorption cross section. For example, the first excitation energy in the optimal gas phase geometry (MP2/cc-pVTZ level) of the CF_2Cl_2 molecule is 7.32 eV (oscillatory strength 0.0176) and it shifts to 7.41 eV (0.0178) in the $CF_2Cl_2\cdots H_2O$ complex and to 7.34 eV (0.0171) in the $CF_2Cl_2\cdots Ar$ complex. In addition, the CFC-12 photodissociation cross section is still large enough in the environment of $(CF_2Cl_2)_n$ and Ar_N clusters. Therefore, we exclude the shift in the photoabsorption cross section as the reason for the missing Cl-fragments.

(3). Cl Fragment Disappearance. If CF_2Cl_2 is present and photolyzed on the cluster, the missing fragment has to disappear in the water cluster or recombine. The first option is that the chlorine radical reacts with water molecules. The reaction $Cl + H_2O \rightarrow HCl + OH$ is endoergic by ≤0.8 eV;[68,69] the HCl formed can further acidically dissociate, decreasing thus the overall reaction energy. The Cl-fragment kinetic energy of ≈1.0 eV after the direct CF_2Cl_2 photodissociation can facilitate this reaction as suggested by theoretical calculations.[70] Yet, in this case we would still expect some of the generated fast Cl fragments to leave the cluster and escape the reaction. Therefore, we can also exclude the Cl reaction. The more probable scenario is that the Cl-fragment is trapped in the ice nanoparticle. The water clusters are more strongly bound compared to the argon clusters. For argon, the deposited energy causes the cluster decay during the dissociation process and the Cl-fragment is released even when it has been slowed to zero energy. On the other hand, the slow chlorine atom cannot be released from the water cluster which remains bound (at least within the duration of the experiment). The third possibility would be a very efficient geminate recombination taking place upon population transfer into the ground electronic state. This again requires an efficient draining of the kinetic energy from the dissociated chlorine atom so that the radical would stay within the first solvation shell and subsequently recombine.

All three scenarios for the fragment disappearance (i.e., the reaction between the chlorine atom and water, chlorine atom trapping, and CF_2Cl_2 recombination) are based on the assumption that there are no dangling C−Cl bonds in the cluster. If the dangling C−Cl bonds were present, the Cl-fragment would be released because the water cluster does not affect the bond. This is demonstrated in Figure 7, showing the

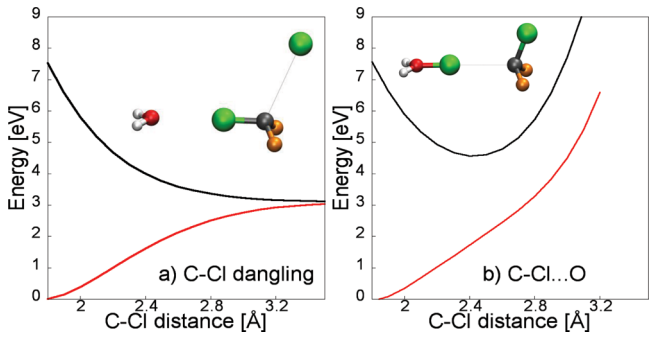

Figure 7. Energy profile along the (a) dangling C−Cl bond and (b) C−Cl···O bond. Ground state (red line) and first singlet excited state (black line) are shown. The calculations were performed at the MR-CI level with a 6-31+g* basis set.

energy profiles for the ground state and the first excited state of the $CF_2Cl_2\cdots H_2O$ complex. The dissociation along (a) the dangling C−Cl bond is characterized by a rapid decrease in energy and fast free dissociation is thus expected. The total excess energy upon the photoabsorption of the 193 nm photon corresponds to 2.9 eV.[19−21] Note that out of this excess energy, only ≈1.0 eV ends up in the form of kinetic energy of the chlorine fragment.[22] The dissociation along (b) the C−Cl···O bond for the C−Cl bond connected to the solvent water molecule (considering the lowest energy structure) is quite different. First, the excess energy is much smaller (∼1.9 eV). Second, the chlorine kinetic energy is transferred into the water molecule. It leaves the static chlorine atom in the proximity of the CF_2Cl radical in a vibrationally highly excited state. Such an arrangement enables a geminate recombination and chlorine atom trapping.

If the CF_2Cl_2 molecule freely rotated on the surface of the spherical ice cluster, dangling C−Cl bonds would be provided and some free Cl fragments would be released. Since such fragments were not observed, we further consider two possibilities: the CF_2Cl_2 molecule is either oriented on the surface with the Cl atoms pointing into the cluster or is embedded inside the cluster. These options are discussed below.

Orientation of CF_2Cl_2 on the Surface. The possible preferential orientation of the CF_2Cl_2 molecule with respect to water particles was tested by computing the structures and relative energies for the various $CF_2Cl_2\cdots H_2O$ arrangements. The rich conformational space of the dimer $CF_2Cl_2\cdots H_2O$ can be divided into 3 distinct binding motifs: halogen bond, hydrogen bond, and dispersion-bound complexes. The representative structures of each motif with the lowest energies are shown in Figure 8. All calculated structures and their energetics can be found in the Supporting Information. The global minimum is represented by a complex in the C−Cl···O arrangement of a halogen bond type (structure **1**). This bond is not nominated a halogen bond accidentally; it displays the major features of halogen bond definition:[71] it is a linear bond with the C−Cl···O bond (3.05 Å) shorter than the sum of van der Waals radii of the Cl (1.75 Å) and O (1.52 Å) atoms. On the other hand, the analogous arrangement of the C−F···O type is almost unbound at the CCSD(T)/CBS level

dx.doi.org/10.1021/jp503983x | J. Phys. Chem. A 2014, 118, 4740−4749

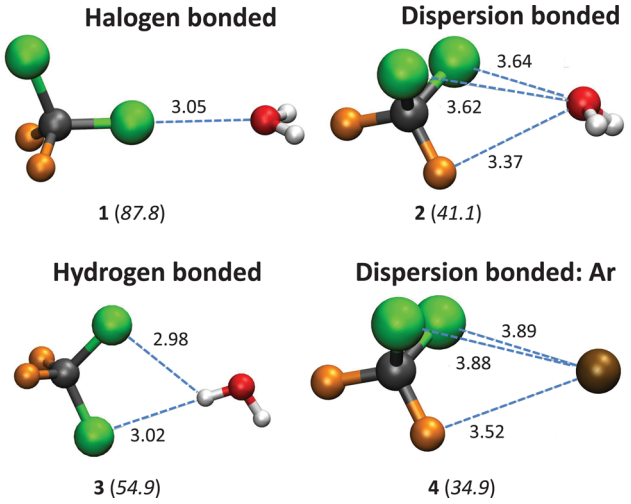

Figure 8. Structures with the highest interaction energies for three distinct $CF_2Cl_2\cdots H_2O$ motifs (**1**, **2**, **3**) and the $CF_2Cl_2\cdots$Ar complex (**4**): interaction energies in millielectron volts (in parentheses), distances in Å. The geometries were obtained at the MP2/cc-pVTZ level; at each minimum, the energies are recalculated at the $CCS_2D(T)$ level in an estimated complete basis set limit. All calculated structures and their energetics can be found in the Supporting Information.

(interaction energy 6 meV, see Figure SI4 of the Supporting Information). This is in line with the general observation that fluorine atoms usually do not form halogen bonds.[29] The halogen bond arrangement should support the orientation of the CFC molecules toward the water surface. The chlorine atom can also act as a hydrogen bond acceptor, which gives rise to the second type of isomers (**3**). The hydrogen-bonded complexes are energetically less favorable by about 40 meV (i.e., half of the interaction energy). Finally, the complexes can be arranged in a structure maximizing dispersion energy (**2**). Such an arrangement is energetically comparable to the hydrogen-bonded complexes. Analogous arrangement, however, represents a global minimum for the $CF_2Cl_2\cdots$Ar complex. Here, the argon atom resides in the center of the ClClF face of the $CFCl_2$ tetrahedron (structure **4**). Only the halogen bond specifically orients the chlorine atoms toward water. We conclude that CF_2Cl_2 could be preferentially oriented on the surface of ice particles. The preference is, however, not very strong, and it is questionable to what extent the halogen bond plays a role on the disordered ice surface.

Embedding of CF_2Cl_2 Inside the Cluster. CF_2Cl_2 is a large molecule, relatively weakly bound to water. Considering the strong hydrogen bonding between water molecules, the direct incorporation of CF_2Cl_2 after the uptake seems unlikely. However, we have recently shown that the shape of the large ice nanoparticles produced in the supersonic expansion is highly irregular and nonspherical.[35] CF_2Cl_2 deposited on the surface can attempt to maximize its interactions, which would position it in the encapsulated sites on the cluster. The photodissociated chlorine atoms would be then efficiently stopped in such an arrangement. Note that, on the other hand, the measurements for argon clusters were found to agree with the spherical nanoparticle shape.

Perspective of Other Experiments. The present analysis of the negative result can be also supported by the comparison with our recent experiments on the photodissoaciation of HCl on water and argon clusters. We have investigated the photodissociation of HCl and other hydrogen halides deposited on Ar_N and $(H_2O)_N$ previously[25,26,28] and repeated these experiments within the present work with the VMI system.

First, the HCl experiments support our claim that the CF_2Cl_2 molecules are, indeed, deposited on $(H_2O)_N$: The mass spectra for HCl pickup on water have similar features to the CF_2Cl_2 case: relatively strong mass peaks corresponding to the molecule and no evidence for $(HCl)_n$ clusters and no mixed HCl/H_2O species. The mass spectra are also similar for the pickup on Ar_N: strong HCl clustering upon multiple pickup (some of the mass spectra can be found in our recent review[30]). We have, however, an independent and unambiguous evidence for the presence of the HCl molecule on the cluster: a strong H-fragment signal from the photodissociation of HCl on $(H_2O)_N$. This analogy shows that the molecules can be deposited on the ice nanoparticles, even though only the molecular peaks are observed in the mass spectra. It is worth mentioning that HCl is not the only additional example, and we have recently studied other molecules which exhibit very similar patterns (e.g., aniline).

There is even a closer analogy between HCl and CF_2Cl_2. Although we detected a strong H-fragment signal from HCl on ice, the corresponding Cl fragments were not observed (both H and Cl fragments were observed from Ar_N). The photodissociation mechanism of HCl on ice clusters is different from the CF_2Cl_2; it proceeds via the photolysis of acidically dissociated HCl with a subsequent formation of H_3O and Cl radicals upon the excitation, as we have shown by series of experiments and theoretical calculations.[25−28] This process can only produce slow Cl fragments, which cannot react with H_2O in the endothermic reaction. Therefore, the Cl fragments are more likely caged mechanically in the nondecaying water clusters. This means that the missing Cl signal can be essentially explained by an immediate production of slow Cl atoms. The geminate recombination between the CF_2Cl and Cl radicals or chlorine reaction with water can take place, such steps are, however, not necessary for the explanation of the experimental observations.

CONCLUSIONS

We have studied CF_2Cl_2 molecule photodynamics on argon and water ice nanoparticles in the complex molecular beam experiment using the velocity map imaging technique. The particle composition was probed by mass spectrometry. The discussion of the results was supported by high-level ab initio calculations. The CF_2Cl_2 photodissociation was explored in different cluster environments: (i) $(CF_2Cl_2)_n$ clusters produced in the coexpansions with Ar buffer gas; (ii) individual CF_2Cl_2 molecules and $(CF_2Cl_2)_n$ clusters deposited on large Ar_N clusters by pickup and coagulation of CF_2Cl_2 molecules; and (iii) CF_2Cl_2 molecules on ice nanoparticles $(H_2O)_N$.

The experimental observations can be summarized as follows: (1) Although the CF_2Cl_2 molecules do not cluster in neat expansions, they readily form $(CF_2Cl_2)_n$ clusters in the coexpansion with Ar buffer gas. (2) The CF_2Cl_2 molecules deposited on large rare gas clusters after multiple pickup coagulate efficiently to $(CF_2Cl_2)_n$ clusters generating $(CF_2Cl_2)_n\cdot Ar_N$ species ($n \approx 1-10$, $N > 10 \times n$). (3) On the other hand, the CF_2Cl_2 molecules do not generate clusters on the $(H_2O)_N$ ice nanoparticles and are adsorbed less efficiently than on argon. (4) Cl fragments from the photodissociation of the CF_2Cl_2 molecules in $(CF_2Cl_2)_n$ clusters are efficiently caged, yet some small direct exit is observed if smaller clusters are formed. (5) Photodissociation of CF_2Cl_2 adsorbed on Ar_N

dx.doi.org/10.1021/jp503983x | J. Phys. Chem. A 2014, 118, 4740−4749

yields only caged Cl fragments. (6) No Cl fragments have been observed from the photodissociation of the CF_2Cl_2 molecules on ice nanoparticles.

From these observations, we emphasize the remarkable energy dissipation observed for the C−Cl dissociation already in $(CF_2Cl_2)_n$ and Ar_N clusters and eventually in $(H_2O)_N$. The rapid slow-down of the chlorine atoms, as opposed to hydrogen fragments, is caused by a comparable mass of the chlorine atoms and the cluster constituents.

Although we proved experimentally that the ice nanoparticles with the CF_2Cl_2 molecules are detected by our mass spectrometer, the lack of the Cl-fragment signal from the photodissociation can still partly be due to the less efficient pickup of CF_2Cl_2 on ice nanoparticles than on Ar_N. In addition, the loss of Cl-fragments on ice nanoparticles can be interpreted by the strong caging: they efficiently loose their kinetic energy in collisions with the cluster constituents, and the slow fragments get trapped in the water cluster which does not decay since it is relatively strongly bound compared to the argon clusters. The almost complete disappearance of the chlorine fragment suggests that CF_2Cl_2 has no dangling C−Cl bonds on the ice surface. This can be explained either by a strong orientation of the adsorbed molecule (possibly via a halogen bond) on the surface or its encapsulation within a cluster of a highly irregular shape.

■ ASSOCIATED CONTENT

Supporting Information

Further experimental mass spectra and calculated complex structures and energies. This material is available free of charge via the Internet at http://pubs.acs.org.

■ AUTHOR INFORMATION

Corresponding Author

*E-mail: michal.farnik@jh-inst.cas.cz. Tel: +420 (0)2 6605 3206. Fax: +420 (0)2 8658 2307.

Notes

The authors declare no competing financial interest.

■ ACKNOWLEDGMENTS

This work has been supported by the Czech Grant Agency project no.: 14-08937S. The authors thank J. Fedor and M. Allan from the University of Fribourg for fruitful discussions and providing CF_2Cl_2 for our experiments.

■ REFERENCES

(1) Solomon, S. Stratospheric Ozone Depletion: A Review of Concepts and History. *Rev. Geophys.* **1999**, *37*, 275−316.

(2) Jacob, D. J. *Introduction to Atmospheric Chemistry*; University Press: Princeton, 1999.

(3) Finlayson-Pitts, B. J.; Pitts, J. N. *Chemistry of the Upper and Lower Atmosphere*; Academic Press: San Diego, 2000.

(4) Lu, Q.-B. Cosmic-Ray-Driven Reaction and Greenhouse Effect of Halogenated Molecules: Culprits for Atmospheric Ozone Depletion and Global Climate Change. *Int. J. Mod. Phys.* **2013**, *27*, 1350073.

(5) Molina, M. J.; Rowland, F. S. Stratospheric Sink for Chlorofluoromethanes: Chlorine Atom-Catalysed Destruction of Ozone. *Nature* **1974**, *249*, 810.

(6) Solomon, S.; Garcia, R. R.; Rowland, F. S.; Wuebbles, D. J. On the Depletion of Antarctic Ozone. *Nature* **1986**, *321*, 755.

(7) Graupner, K.; Haughey, S. A.; Field, T. A.; Mayhew, C. A.; Hoffmann, T. H.; May, O.; Fedor, J.; Allan, M.; Fabrikant, I. I.; Illenberger, E.; et al. Low-Energy Electron Attachment to the Dichlorodifluoromethane (CCl_2F_2) Molecule. *J. Phys. Chem. A* **2010**, *114*, 1474−1484.

(8) Lu, Q.-B.; Madey, T. E. Giant Enhancement of Electron-Induced Dissociation of Chlorofluorocarbons Coadsorbed with Water or Ammonia Ices: Implications for Atmospheric Ozone Depletion. *J. Chem. Phys.* **1999**, *111*, 2861.

(9) Lu, Q.-B.; Sanche, L. Effects of Cosmic Rays on Atmospheric Chlorofluorocarbon Dissociation and Ozone Depletion. *Phys. Rev. Lett.* **2001**, *87*, 078501.

(10) Lu, Q.-B. Cosmic-Ray-Driven Electron-Induced Reactions of Halogenated Molecules Adsorbed on Ice Surfaces: Implications for Atmospheric Ozone Depletion and Global Climate Change. *Phys. Rep.* **2010**, *487*, 141−167.

(11) Bertin, M.; Meyer, M.; Stähler, J.; Gagl, C.; Wolf, M.; Bovensiepen, U. Reactivity of Water-Electron Complexes on Crystalline Ice Surfaces. *Faraday Discuss.* **2009**, *141*, 293−307.

(12) Lu, Q.-B.; Sanche, L. Enhanced Dissociative Electron Attachment to CF_2Cl_2 by Transfer of Electrons in Precursors to the Solvated State in Water and Ammonia Ice. *Phys. Rev. B* **2001**, *63*, 153403.

(13) Lu, Q.-B.; Sanche, L. Dissociative Electron Attachment to CF_4, CFCs and HCFCs Adsorbed on H_2O Ice. *J. Chem. Phys.* **2004**, *120*, 2434.

(14) Yabushita, A.; Inoue, Y.; Senga, T.; Kawasaki, M.; Sato, S. Photodissociation of Chlorine Molecules Adsorbed on Amorphous and Crystalline Water Ice Films. *J. Phys. Chem. B* **2002**, *106*, 3151−3159.

(15) Yabushita, A.; Kawasaki, M.; Sato, S. Ultraviolet Photodissociation Dynamics of Cl_2 and $CFCl_3$ Adsorbed on Water Ice Surfaces. *J. Phys. Chem. A* **2003**, *107*, 1472−1477.

(16) Perry, C. C.; Wolfe, G. M.; Wagner, A. J.; Torres, J.; Faradzev, N. S.; Madey, T. E.; Fairbrother, D. H. Chemical Reactions in CF_2Cl_2/Water (Ice) Films Induced by X-ray Radiation. *J. Phys. Chem. B* **2003**, *107*, 12740−12751.

(17) Perry, C. C.; Faradzev, N. S.; Fairbrother, D. H.; Madey, T. H. Electron Stimulated Reactions of Halogenated Compounds in Condensed Phases: Effects of Solvent Matrices on Reaction Dynamics and Kinetics. *Int. Rev. Phys. Chem.* **2004**, *23*, 289−340.

(18) Matsumi, Y.; Tonokura, K.; Kawasaki, M.; Inoue, G.; Satyapal, S.; Bersohn, R. Fine Structure Branching Ratios and Doppler Spectroscopy of Chlorine Atoms from the Photodissociation of Alkyl Chlorides and Chlorofluoromethanes at 157 and 193 nm. *J. Chem. Phys.* **1991**, *94*, 2669.

(19) Baum, G.; Huber, J. R. Photodissociation of CF_2Cl_2 at 193 nm Investigated by Photofragment Spectroscopy. *Chem. Phys. Lett.* **1993**, *203*, 261.

(20) Yen, M.; Johnson, P. M.; White, M. G. The Vacuum Ultraviolet Photodissociation of the Chlorofluorocarbons. Photolysis of CF_3Cl, CF_2Cl_2, and $CFCl_3$ at 187, 125, and 118 nm. *J. Chem. Phys.* **1993**, *99*, 126.

(21) Taketani, F.; Takahashi, K.; Matsumi, Y. Quantum Yields for $Cl(^2P_j)$ Atom Formation from the Photolysys of Chlorofluorocarbons and Chlorinated Hydrocarbons at 193.3 nm. *J. Phys. Chem. A* **2005**, *109*, 2855.

(22) Poterya, V.; Kočišek, J.; Pysanenko, A.; Fárník, M. Caging of Cl Atoms from Photodissociation of CF_2Cl_2 in Clusters. *Phys. Chem. Chem. Phys.* **2014**, *16*, 421−429.

(23) Fárník, M.; Nahler, N. H.; Buck, U.; Slavíček, P.; Jungwirth, P. Photodissociation of HBr on the Surface of Ar_n Clusters at 193 nm. *Chem. Phys.* **2005**, *315*, 161.

(24) Fedor, J.; Kočišek, J.; Poterya, V.; Votava, O.; Pysanenko, A.; Lipciuc, L.; Kitsopoulos, T. N.; Fárník, M. Velocity Map Imaging of HBr Photodissociation in Large Rare Gas Clusters. *J. Chem. Phys.* **2011**, *134*, 154303.

(25) Poterya, V.; Fárník, M.; Slavíček, P.; Buck, U.; Kresin, V. V. Photodissociation of Hydrogen Halide Molecules on Free Ice Nanoparticles. *J. Chem. Phys.* **2007**, *126*, 071101.

(26) Ončák, M.; Slavíček, P.; Poterya, V.; Fárník, M.; Buck, U. Emergence of Charge-Transfer-to-Solvent Band in the Absorption Spectra of Hydrogen Halides on Ice Nanoparticles: Spectroscopic

Evidence for Acidic Dissociation. *J. Phys. Chem. A* **2008**, *112*, 5344−5353.
(27) Poterya, V.; Fedor, J.; Pysanenko, A.; Tkáč, O.; Lengyel, J.; Ončák, M.; Slavíček, P.; Fárník, M. Photochemistry of HI on Argon and Water Nanoparticles: Hydronium Radical Generation in HI·$(H_2O)_N$. *Phys. Chem. Chem. Phys.* **2011**, *13*, 2250−2258.
(28) Ončák, M.; Slavíček, P.; Fárník, M.; Buck, U. Photochemistry of Hydrogen Halides on Water Clusters: Simulations of Electronic Spectra and Photodynamics, and Comparison with Photodissociation Experiments. *J. Phys. Chem. A* **2011**, *115*, 6155−6168.
(29) Metrangolo, P.; Neukirch, H.; Pilati, T.; Resnati, G. Halogen Bonding Based Recognition Processes: A World Parallel to Hydrogen Bonding. *Acc. Chem. Res.* **2005**, *38*, 386−395.
(30) Fárník, M.; Poterya, V. Atmospheric Processes on Ice Nanoparticles in Molecular Beams. *Front. Chem.* **2014**, *2*, 4.
(31) Lengyel, J.; Pysanenko, A.; Kočišek, J.; Poterya, V.; Pradzynski, C.; Zeuch, T.; Slavíček, P.; Fárník, M. Nucleation of Mixed Nitric Acid-Water Ice Nanoparticles in Molecular Beams that Starts with a HNO_3 Molecule. *J. Phys. Chem. Lett.* **2012**, *3*, 3096.
(32) Kočišek, J.; Lengyel, J.; Fárník, M.; Slavíček, P. Energy and Charge Transfer in Ionized Argon Coated Water Clusters. *J. Chem. Phys.* **2013**, *139*, 214308.
(33) Fedor, J.; Poterya, V.; Pysanenko, A.; Fárník, M. Cluster Cross Sections from Pickup Measurements: Are the Established Methods Consistent? *J. Chem. Phys.* **2011**, *135*, 104305.
(34) Lengyel, J.; Kočišek, J.; Poterya, V.; Pysanenko, A.; Svrčková, P.; Fárník, M.; Zaouris, D.; Fedor, J. Uptake of Atmospheric Molecules by Ice Nanoparticles: Pickup Cross Sections. *J. Chem. Phys.* **2012**, *137*, 034304.
(35) Lengyel, J.; Pysanenko, A.; Poterya, V.; Slavíček, P.; Fárník, M.; Kočišek, J.; Fedor, J. Irregular Shapes of Water Clusters Generated in Supersonic Expansions. *Phys. Rev. Lett.* **2014**, *112*, 113401-1−113401-5.
(36) Fárník, M. *Molecular Dynamics in Free Clusters and Nanoparticles Studied in Molecular Beams*; ICT Prague Press: Prague, 2011.
(37) Fárník, M.; Poterya, V.; Kočišek, J.; Fedor, J.; Slavíček, P. Short Review on the Acetylene Photochemistry in Clusters: Photofragment Caging and Reactivity. *Mol. Phys.* **2012**, *110*, 2817.
(38) Whitaker, B. *Imaging in Molecular Dynamics: Technology and Applications*; Cambridge University Press: Cambridge, 2003.
(39) Kaesdorf, S. *Geräte für Forschung und Industrie*; Wiley: Munich, 2011.
(40) Kočišek, J.; Lengyel, J.; Fárník, M. Ionization of Large Homogeneous and Heterogeneous Clusters Generated in Acetylene-Ar Expansions: Cluster Ion Polymerization. *J. Chem. Phys.* **2013**, *138*, 124306.
(41) Hagena, O. F. Nucleation and Growth of Clusters in Expanding Nozzle Flows. *Surf. Sci.* **1981**, *106*, 101.
(42) Hagena, O. F. Condensation in Free Jets: Comparison of Rare Gases and Metals. *Z. Phys. D* **1987**, *4*, 291.
(43) Hagena, O. F. Cluster Ion Sources. *Rev. Sci. Instrum.* **1992**, *63*, 2374.
(44) Buck, U.; Krohne, R. Cluster Size Determination from Diffractive He Atom Scattering. *J. Chem. Phys.* **1996**, *105*, 5408.
(45) Bobbert, C.; Schütte, S.; Steinbach, C.; Buck, U. Fragmentation and Reliable Size Distributions of Large Ammonia and Water Clusters. *Eur. Phys. J. D* **2002**, *19*, 183−192.
(46) Boys, S.; Bernardi, F. The Calculation of Small Molecular Interactions by the Differences of Separate Total Energies. Some Procedures with Reduced Errors. *Mol. Phys.* **1970**, *19*, 553−566.
(47) Řezáč, J.; Riley, K. E.; Hobza, P. Evaluation of the Performance of Post-Hartree-Fock Methods in Terms of Intermolecular Distance in Noncovalent Complexes. *J. Comput. Chem.* **2012**, *33*, 691−694.
(48) Řezáč, J.; Riley, K. E.; Hobza, P. S66: A Well-Balanced Database of Benchmark Interaction Energies Relevant to Biomolecular Structures. *J. Chem. Theory Comput.* **2011**, *7*, 2427−2438.
(49) Werner, H.-J.; Knowles, P. J.; Knizia, G.; Manby, F. R.; Schütz, M. Molpro: a General-Purpose Quantum Chemistry Program Package. *Wiley Interdiscip. Rev.: Comput. Mol. Sci.* **2012**, *2*, 242−253.
(50) Werner, H.-J.; Knowles, P. J.; Knizia, G.; Manby, F. R.; Schütz, M.; et al. *MOLPRO*, version 2010.1, A Package of Ab Initio Programs; 2010 (http://www.molpro.net).
(51) Frisch, M. J. et al. *Gaussian 09*, revision A.1. Gaussian Inc.: Wallingford, CT, 2009.
(52) Malakhovskii, A. V.; Ben-Zion, M. Temporal Evolution of an Argon Cluster During the Process of its Evaporation. *Chem. Phys.* **2001**, *264*, 135−143.
(53) Temelso, B.; Archer, K. A.; Shields, G. C. Benchmark Structures and Binding Energies of Small Water Clusters with Anharmonicity Corrections. *J. Phys. Chem. A* **2011**, *115*, 12034−12046.
(54) Ogilvie, J. F.; Wang, F. Y. H. Potential-Energy Functions of Diatomic Molecules of the Noble Gases I. Like Nuclear Species. *J. Mol. Struct.* **1992**, *273*, 277.
(55) Baumfalk, R.; Buck, U.; Frischkorn, C.; Gandhi, S. R.; Lauenstein, C. UV Photolysis of $(HBr)_n$ Clusters with Known Size Distribution. *Chem. Phys. Lett.* **1997**, *269*, 321.
(56) Baumfalk, R.; Buck, U.; Frischkorn, C.; Gandhi, S. R.; Lauenstein, C. Photodissociation and Size Analysis of $(HBr)_n$ Clusters. *Ber. Bunsenges. Phys. Chem.* **1997**, *101*, 606.
(57) Baumfalk, R.; Nahler, N. H.; Buck, U. Vibrational Excitation and Caging Following the Photodissociation of Small HBr Clusters in and on Large Ar Clusters. *Phys. Chem. Chem. Phys.* **2001**, *3*, 2372.
(58) Buck, U. Photodissociation of Hydrogen Halide Molecules in Different Cluster Environments. *J. Phys. Chem. A* **2002**, *106*, 10049.
(59) Nahler, N. H.; Baumfalk, R.; Buck, U.; Vach, H.; Slavíček, P.; Jungwirth, P. Photodissociation of HBr in and on Ar_n Clusters: The Role of the Position of the Molecule. *Phys. Chem. Chem. Phys.* **2003**, *5*, 3394.
(60) Nahler, N. H.; Fárník, M.; Buck, U.; Vach, H.; Gerber, R. B. Photodissociation of HCl and Small $(HCl)_m$ Complexes in and on Large Ar_n Clusters. *J. Chem. Phys.* **2004**, *121*, 1293.
(61) Slavček, P.; Jungwirth, P.; Lewerenz, M.; Nahler, N. H.; Fárník, M.; Buck, U. Photodissociation of HI on the Surface of Large Argon Clusters: The Orientation of Librational Wavefunction and the Scattering from the Cluster Cage. *J. Chem. Phys.* **2004**, *120*, 4498.
(62) Lu, Q.-B.; Madey, T. E.; Parenteau, L.; Weik, F.; Sanche, L. Structural and Temperature Effects on Cl-Yields in Electron-Induced Dissociation of CF_2Cl_2 Adsorbed on Water Ice. *Chem. Phys. Lett.* **2001**, *342*, 1−6.
(63) Jansen, R.; Wysong, I.; Gimelshein, S.; Zeifman, M.; Buck, U. Non-equilibrium Numerical Model of Homogeneous Condensation in Argon and Water Vapour Expansions. *J. Chem. Phys.* **2010**, *132*, 244105.
(64) Pradzynski, C. C.; Forck, R. M.; Zeuch, T.; Slavíček, P.; Buck, U. A Fully Size-Resoved Perspective on the Crystallization of Water Clusters. *Science* **2012**, *337*, 1529−1532.
(65) Buck, U.; Pradzynski, C. C.; Zeuch, T.; Dieterich, J. M.; Hartke, B. A Size Resolved Investigation of Large Water Clusters. *Phys. Chem. Chem. Phys.* **2014**, *16*, 6859−6871.
(66) Biham, O.; Furman, I.; Pirronello, V.; Vidali, G. Master Equation for Hydrogen Recombination on Grain Surfaces. *Astrophys. J.* **2001**, *553*, 595−603.
(67) This energy has been estimated approximately as 3−4 times the calculated binding energy of $CF_2Cl_2\cdots H_2O$.
(68) Sinha, A.; Thoemke, J. D.; Crim, F. F. Controlling Bimolecular Reactions: Mode and Bond Selected Reaction of Water with Translationally Energetic Chlorine Atoms. *J. Chem. Phys.* **1992**, *96*, 372−376.
(69) Thoemke, J. D.; Pfeiffer, J. M.; Metz, R. B.; Crim, F. F. Mode- and Bond-Selective Reactions of Chlorine Atoms with Highly Vibrationally Excited H_2O and HOD. *J. Phys. Chem.* **1995**, *99*, 13748−13754.
(70) Rougeau, N. Planar Study of $H_2O + Cl \rightarrow HO + HCl$ Reactions. *Phys. Chem. Chem. Phys.* **2007**, *9*, 2113−2120.
(71) Desiraju, G. R.; Ho, P. S.; Kloo, L.; Legon, A. C.; Marquardt, R.; Metrangolo, P.; Politzer, P.; Resnati, G.; Rissanen, K. Definition of the Halogen Bond. *Pure Appl. Chem.* **2013**, *85*, 1711−1713.